MODELLING OF SHORT AND LONG TERM PROPERTIES OF VBR MPEG COMPRESSED VIDEO IN ATM NETWORKS

Jürgen Enssle
Institute of Communications Switching and Data Technics
University of Stuttgart
Seidenstraße 36, 70174 Stuttgart, Germany, NC-012

ABSTRACT

The future Broadband Integrated Services Digital Network (B-ISDN) will be based on the Asynchronous Transfer Mode (ATM) that allows statistical multiplexing of variable bitrate (VBR) sources. Video data will have a major share in future broadband traffic. In this paper we investigate in detail the short and long term statistical properties of video sequences encoded according to the MPEG-1 video coding standard. A flexible hierarchical stochastic source model will be presented that can be matched to the properties of any MPEG encoded video sequence. The model takes the first and second order statistical properties and the short and long term correlation characteristics into account, including long range dependence (LRD) effects. The performance of an ATM multiplexer fed by a number of MPEG video sources is evaluated and used to validate the simulation models.

INTRODUCTION

The Asynchronous Transfer Mode (ATM) has been standardised for the future Broadband-ISDN (Integrated Services Digital Network). It has to cope with a vast variety of services with different bitrate and QoS (Quality of Service) requirements. The ATM principle is based on the transfer of packets with constant length allowing statistical multiplexing. But with this, different connections may influence each other in the QoS they perceive. The ATM QoS can be expressed in terms of cell losses, cell delays and cell delay variations whereof in this paper we will focus on cell losses.

In order to investigate the impact of different traffic sources and associated services on the network, models are necessary that characterise the statistical properties and the behavior of the sources and associated ATM traffic streams. Thus, the development of video source models and their validation is essential for performance analyses. Via the introduction of video on demand services, conferencing services and as a main constituent of multimedia applications, video data will have a major share in future broadband traffic. Generally, the behavior of a video source and thus its statistical characteristics depend on the coding technique, the application and the video contents.

Previous studies on the characterisation of VBR video sources were based on a variety of coding techniques [Garr 91, Magl 88, MRSZ 92, NFO 89, RaSe 90, SSD 93, VPV 88]. But the important statistics and results obtained by these studies have to be extended for more complex coding techniques such as MPEG-1 (Motion Pictures Experts Group), that was standardised by ISO/IEC (International Organization for Standardization, International Electrotechnical Commission) in 1992 [MPEG 92]. In [PaZa 92, PaZa 93] the effect of two main parameters on the video statistics and variable bandwidth allocation schemes were investigated based on a 3 minute 40 second sequence. Four CCIR601 test video sequences, 2000 frames in total, were studied and used for a multiplexing analysis in [Rein 93].

This paper analyses the properties of VBR (Variable Bit Rate) MPEG-1 encoded video data and their behavior in an ATM environment. A very long sequence (about 82 minutes) of the movie "Starwars" and a sequence of about 24 minutes of "CNN News" were encoded using a distributed MPEG-1 software encoder and frame statistics traces were extracted for different picture sizes.

The statistical properties of a VBR video data stream at different time scales depend on various factors. At

the cell level, the packetization process is dominant. At the picture level, the behavior of the encoder, its parameters and algorithms are essential. The fluctuations in the amount of information in consecutive pictures at the scene level are governed by the contents and type of video material independent of the used coding algorithm. To take all these facts into account, a flexible hierarchical stochastic source model for simulation purposes was developed that can provide different levels of complexity adjustable to the requirements of the system under investigation. In [GaWi 94] strong evidence for the presence of long range dependence (LRD) was found in the VBR video statistics trace presented in [Garr 91]. The LRD property is mainly due to the different complexity of consecutive pictures and scenes. These properties will be represented in our model at the scene level by the use of an approximation of discrete fractional Gaussian noise (dfGn) called fast fractional Gaussian noise (ffGn) [Mand 71]. The characteristics of the MPEG encoding algorithm will be modelled at the picture level by suitable transformations of the scene level random process.

The remaining of the paper is organized as follows: First, we will briefly describe the main characteristics of the MPEG encoding algorithm that will be reflected in the source model. Then, fractional Gaussian noise processes and analysis methods to assess their properties will be described. Next, a hierarchical source model will be introduced and the algorithms that are used at the different levels will be described. Thereafter, the performance of the source model is compared with that of the empirical statistics traces by simulation of the behavior of a deterministic multiplexer with finite buffer fed by several VBR video sources. Finally, the main results will be presented and conclusions will be given.

VBR MPEG ENCODED VIDEO

The MPEG-1 video coding standard uses a combination of intra- and interframe coding because of the conflicting requirements of random access and highly efficient compression. The color difference signals of the digitized input signal are subsampled with respect to the luminance by 4:1:1 to match the sensitivity of the human visual system. The use of motion compensation allows to exploit temporal redundancy in the video sequence. Spatial and perceptual redundancy reduction is achieved via Discrete Cosine Transform (DCT) coding on 8 $\times$ 8 pixel blocks and quantization of the DCT coefficients. After the quantization two-dimensional run-length coding is used to encode the quantized DCT coefficients.

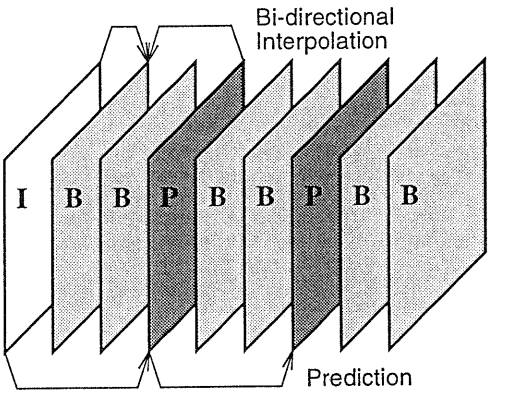

Figure 1: Temporal picture pattern ($N = 9$, $M = 3$)

Three main picture types are defined. Intra coded pictures (I-pictures) are coded without reference to other pictures. Predictive coded pictures (P-pictures) are coded more efficiently using motion compensated prediction from a past I- or P-picture. Bidirectionally-predictive coded pictures (B-pictures) provide the highest degree of compression using past and future I- or P-pictures as a reference for motion compensation [MPEG 92]. The three picture types are organized in a so called group of pictures (GOP) defined by the distance N between I-pictures and the distance M between P-pictures. The GOP structure we used is IBBPBBPBB with $N = 9$ and $M = 3$ (Figure 1).

To investigate the behavior and statistical properties of MPEG encoded video data and as a basis for the parametrisation of our model, we encoded a very long sequence of the movie 'Starwars' and a sequence of 'CNN News' using a distributed encoding environment based on the Berkeley MPEG-1 encoder version 1.1. The picture size was set to 640 $\times$ 480 pixel at a picture rate of 25 Hz. The sequence lengths of the statistics traces containing the number of bits necessary to encode the pictures are 123574 and 36664 pictures, respectively. The basic statistical properties of the traces are listed in Table 1.

Picture type	Minimum [*bit*]	Maximum [*bit*]	Mean [*bit*]	Coefficient of variation
Starwars				
I	44520	387656	$1.82 \cdot 10^5$	0.24
P	14352	394920	$1.03 \cdot 10^5$	0.33
B	2720	144048	$4.41 \cdot 10^4$	0.32
All	2720	394920	$7.25 \cdot 10^4$	0.72
CNN News				
I	40480	514432	$2.37 \cdot 10^5$	0.26
P	9152	471048	$1.04 \cdot 10^5$	0.43
B	936	191072	$3.89 \cdot 10^4$	0.42
All	936	514432	$7.51 \cdot 10^4$	0.94

Table 1: Picture size statistics

The raw material for the 'Starwars' statistics trace was taken from a laser disk, whereas the 'CNN News' sequence was recorded from the cable television network with a VCR. Since the cable television signal contains more noise than that of the laser disk, the overall bitrate of the 'CNN News' trace is higher and the coefficients of variation are larger compared to those of the 'Starwars' trace.

FRACTIONAL GAUSSIAN NOISE PROCESSES AND LONG RANGE DEPENDENCE

It has been discovered [GaWi 94] that in discrete time series $\{X_t\}$, $t = 1, 2, \ldots, n$, of consecutive picture sizes in VBR video traces even observations a long time span apart are significantly dependent. This is in contrast to the common assumption in time series modelling that observations a long time span apart are nearly independent. This statistical property is called long range dependence (LRD), "persistence" or the "Hurst effect". It was first discovered in natural time series like river levels and precipitation records in hydrology by H. E. Hurst [Hurs 51] and is quantified via the Hurst parameter H, $0 \leq H \leq 1$. Formally, persistence can be characterised in several ways [Hosk 84, Cox 84]:

1. by a correlation function that decays hyperbolically as the lag increases, i.e. the sum of the correlation coefficients tends to infinity as the number of considered lags tends to infinity.

2. by a variance of the aggregated process

$$X_t^{(m)} = (X_{tm-m+1} + \ldots + X_{tm})/m$$

that behaves corresponding to

$$\text{VAR}\left[X_t^{(m)}\right] \approx m^{-(2-2H)} \text{VAR}\,[X_t].$$

3. by a spectral density function (periodogram) $I_{n,X}$ that increases without limit as the frequency tends to zero.

4. by the rescaled adjusted range $R(t, s)$, that behaves like n^H, $H > 0.5$ instead of $n^{0.5}$ characteristic for short memory processes.

Since the periodogram analysis and the rescaled adjusted range (R/S) analysis will be used in the sequel to estimate the LRD present in VBR MPEG video sequences and evaluate their Hurst parameter H, the basic equations defining these quantities will be given next. Then, the equations defining fast fractional Gaussian noise, an approximation of discrete fractional Gaussian noise will be given (adopted from [MaWa 69a] and [Mand 71]).

Periodogram Analysis

The empirical periodogram of a stationary time series, given a sample of n observations, $\{X_t\}$, $t = 1, 2, \ldots, n$, can be computed using the fast Fourier transform. First, a centered time series $\{Y_t\}$ with $\text{E}[Y_t] = 0$ is derived from $\{X_t\}$ by

$$Y_t = X_t - \text{E}[X_t] \quad \text{for} \quad t = 1, \ldots, n \qquad (1)$$

with

$$\mathrm{E}[X_t] = \frac{1}{n}\sum_{t=1}^{n} X_t \, .$$

The discrete Fourier transform of the time series $\{Y_t\}$ for $t = 1, \ldots, n$ is defined by

$$\zeta_Y(\omega_k) = \sum_{t=1} n Y_t e^{-j\omega_k t} \qquad (2)$$

over the discrete set of frequencies

$$\omega_k = \frac{2\pi k}{n} \, , \qquad k = 0, \pm 1, \ldots, \pm\lfloor n/2 \rfloor \, .$$

To calculate the discrete Fourier transform, the fast Fourier transform algorithm can be used. The periodogram (unbiased estimate of the nonnormalized spectral density function) of the centered time series $\{Y_t\}$ is defined as

$$I_{n,Y}(\omega_k) = \frac{1}{2\pi n}|\zeta_Y(\omega_k)|^2 \, . \qquad (3)$$

The use of the centered data $\{Y_t\}$ does not affect the asymptotic sampling properties of the periodogram for $\omega_k \neq 0$ and it is $I_{n,X}(\omega_k) \equiv I_{n,Y}(\omega_k)$ whereas for $\omega_k = 0$ it is $I_{n,Y}(\omega_k) = 0$, but $I_{n,X}(\omega_k) = \frac{n}{2\pi}\mathrm{E}[X_t]$.

Rescaled Adjusted Range Analysis

A profound discussion of the application of the rescaled adjusted range to evaluate the LRD properties of a time series $\{X_t\}$, called R/S analysis, is given in [MaWa 69a, part 2] and [MaWa 69b]. It is based on the rescaled adjusted range statistics originally introduced in [Hurs 51]. Here we only want to state its definition and explain its application to estimate the Hurst parameter H of a time series.

Given $X^*(t) = \sum_{u=1}^{t} X(u)$ and an integer s, the expression

$$\begin{aligned} R(t,s) = \\ = \max_{0\le u\le s}\Big[X^*(t+u) - X^*(t) - \\ - \frac{u}{s}(X^*(t+s) - X^*(t))\Big] - \\ - \min_{0\le u\le s}\Big[X^*(t+u) - X^*(t) - \\ - \frac{u}{s}(X^*(t+s) - X^*(t))\Big] \end{aligned} \qquad (4)$$

is called the sample sequential range of $X(t)$ for the lag s. The sequential variance $S^2(t,s)$ is defined by

$$\begin{aligned} S^2(t,s) = \\ = \frac{1}{s}\sum_{u=1}^{s}\Big[X(t+u) - \frac{1}{s}\left[X^*(t+s) - X^*(t)\right]\Big]^2 \, . \end{aligned} \qquad (5)$$

Finally, the rescaled adjusted range statistic is defined as $R(t,s)/S(t,s)$. Hurst showed empirically, that for many naturally occurring time series the expectation of $R(t,s)/S(t,s)$ follows a power law [Hurs 51], i.e.,

$$E\left[R(t,s)/S(t,s)\right] \approx s^H \quad \text{as} \quad s \to \infty \, , \qquad (6)$$

with $0.5 < H < 1$ whereas it was shown independently by Hurst and Feller [Hurs 51, Fell 51] that for a purely random normal process it is $E\left[R(t,s)/S(t,s)\right] = \sqrt{(s\pi/2)}$ for large s.

A practical implementation of the R/S analysis to estimate the Hurst parameter H of an empirical time series trace of length n is proposed in [WaMa 70]. The time series trace is partitioned into a number of subsequences. Now the rescaled adjusted range is calculated for all subsequences (different t) and all possible s that are equally spaced in a logarithmic scale. In a 'pox diagram' all points defining the relation $\log(R(t,s)/S(t,s))$ versus $\log(s)$ are plotted. A line is fitted through all these points for $s_0 \le s \le n$ by the method of least squares. s_0 has to be evaluated subjectively to delete nonlinear relations of $\log(R(t,s)/S(t,s))$ versus $\log(s)$ for small values of s resulting from the short term correlation structure of the trace. The slope of the fitted line is an estimate of the Hurst parameter H.

Fractional Gaussian Noises

In [GaWi 94] and [Hosk 84] ARIMA processes, generalised by fractional differencing, are used to generate persistent time series. The major drawback of the algorithm to generate these processes is that each sample depends on every previous sample, thus the generation of n samples requires $o(n^2)$ computation time. This renders simulations more difficult. Thus, in our studies we used an implementation of a fast fractional Gaussian noise (ffGn) process to generate persistent time series. ffGn processes are an approximation of discrete fractional Gaussian noise (dfGn) processes, that still exhibit the desired LRD property over a certain time interval, but are far simpler to use for simulation purposes. These processes and their properties are discussed in detail in [MaWa 69a, part 3] and [Mand 71]. In the following we will repeat the basic equations defining the dfGn and ffGn processes.

The main property of a continuous Brownian motion random process (Bachelier process, Wiener process) $B(t)$ is that, for every $\epsilon > 0$, the sequence of increments $B(t+\epsilon)-B(t)$ with t an integer multiple of ϵ is a sequence of independent Gaussian random variables with zero mean and variance equal to ϵ. The fractional Brownian motion random process $B_H(t)$ is deduced from the continuous Brownian motion random process by

$$\begin{aligned} B_H(t) - B_H(0) &= \\ &= \int_{-\infty}^{0} \left[(t-u)^{H-0.5} - (-u)^{H-0.5}\right] dB(u) + \\ &+ \int_{0}^{t} (t-u)^{H-0.5}\, dB(u)\ . \end{aligned} \tag{7}$$

This function $B_H(t) - B_H(0)$ exists if and only if $0 < H < 1$. For $H = 0.5$ fractional Brownian motion reduces to ordinary Brownian motion, so it can be regarded as a generalisation of the latter. The increments $B_H(t) - B_H(t-\epsilon)$ with t an integer multiple of ϵ constitute a stationary random process. The sequence of values $B_H(t) = B_H(t) - B_H(t-1)$ is called 'discrete-time fractional Gaussian noise' and is deduced from continuous Brownian motion by

$$B_H(t) = \int_{-\infty}^{t} K_H(t-u)\, dB(u) \tag{8}$$

with the 'kernel function' $K_H(u)$ given by

$$K_H(u) = \begin{cases} u^{H-0.5} & 0 < u < 1 \\ u^{H-0.5} - (u-1)^{H-0.5} & 1 < u \end{cases}\ . \tag{9}$$

For $H = 0.5$, $B_H(t)$ reduces to a discrete-time Gaussian white noise with $\epsilon = 1$. The autocorrelation coefficient $r\left[B_H(t), B_H(t)^{(s)}\right]$ is calculated for $s > 0$ ($r\left[B_H(t), B_H(t)^{(0)}\right] = 1$) according to

$$\begin{aligned} r\left[B_H(t), B_H(t)^{(s)}\right] &= \\ &= \frac{1}{2}\left[(s+1)^{2H} - 2s^{2H} + (s-1)^{2H}\right] \end{aligned} \tag{10}$$

From equation (10) it can be seen that dfGn exhibits the desired hyperbolically decaying autocorrelation coefficient required for an LRD process, but it is defined via an integral that is not very much suited for simulation purposes on a computer. Therefore ffGn, an approximation of dfGn, that only needs $o(n)$ computation time to generate a time series of n observations will be introduced next (adopted from [Mand 71]). Basically, the ffGn process $X_f(t,H)$ consists of a finite sum of Markov-Gauss processes approximating the autocorrelation function of the dfGn process. In the following we will restrict ourselves to ffGn with zero mean and unit variance, since this will be the basis of the VBR MPEG source model that will be presented later. The ffGn process is constructed as the sum of a low frequency term $X_l(t,H)$ and a high frequency term $X_h(t,H)$, i.e.

$$X_f(t,H) = X_l(t,H) + X_h(t,H)\ . \tag{11}$$

Besides the parameters t and H two additional convenience parameters are required, the base B and the quality Q. As $B \to 1$ and $Q \to \infty$ the approximation of the dfGn autocorrelation coefficient by the low frequency term will improve. The low frequency

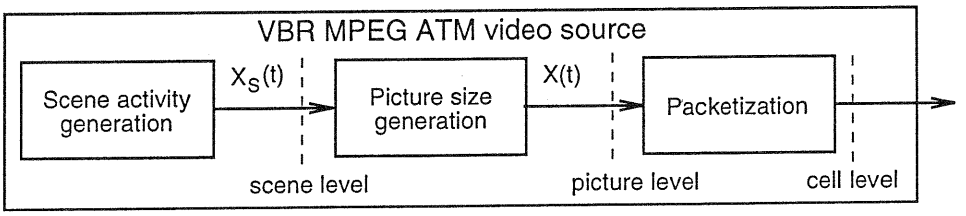

Figure 2: ATM MPEG video source model

term is defined as the weighted sum of $N(n)$ independent Markov-Gauss processes $X(t, r_k|\, MG)$ with zero mean, unit variance and covariance r_k^s

$$X_l(t,H) = \sum_{k=1}^{N(n)} W_k X(t, r_k|\, MG)\ . \qquad (12)$$

The weight factors W_k are determined by

$$W_k^2 = \frac{H(2H-1)\left(B^{1-H} - B^{H-1}\right)}{\Gamma(3-2H)} B^{-2k(1-H)} \qquad (13)$$

and the lag-1 covariance is given by

$$r_k = e^{-B^{-k}}\ . \qquad (14)$$

The number of Markov-Gauss processes $N(n)$ depends on the desired length n of the time series and the convenience parameters B and Q and is calculated according to

$$N(n) = \lceil \ln(Qn)/\ln(B) \rceil\ , \qquad (15)$$

where $\lceil x \rceil$ denotes the smallest integer larger than x. The Markov-Gauss processes $X(t, r_k|\, MG)$ are defined by

$$X(t, r_k|\, MG) = \\ = \begin{cases} G_k(1) & t = 1 \\ r_k\, X(t-1, r_k|\, MG) + \\ +sqrt(1-r_k^2)\, G_k(t) & t > 1 \end{cases} \qquad (16)$$

with $G_k(t)$, $k = 1, \ldots, N(n)$ being sequences of Gaussian variables of zero mean and unit variance (discrete-time white Gaussian noises).

The high frequency term generally may be a Markov-Gauss process to ensure that the ffGn process has unit variance and a lag-1 correlation of $2^{2H-1} - 1$ corresponding to the lag-1 correlation of the dfGn. In our case it is sufficient to use a simple Gauss process that guarantees that the ffGn process has unit variance, since the MPEG encoding algorithm heavily influences the short term correlation of the VBR MPEG video data stream, thus it is not necessary to exactly reproduce the lag-1 correlation of the dfGn process. So the high frequency term $X_h(t,H)$ is calculated according to

$$X_h(t,H) = \sqrt{1 - \frac{B^{H-1}}{4(1-H)\Gamma(-2H)}}\, G(t)\ , \qquad (17)$$

where $G(t)$ is a sequence of Gaussian variables of zero mean and unit variance.

MODELLING

Within this section we will introduce the general structure of the hierarchical VBR MPEG video source model and a simple model of an ATM multiplexer fed by a number of such video sources. The algorithms and transformations used at its different levels will be presented and the analysis methods described in the previous section will be applied to extract the necessary parameters from the empirical statistics traces.

Hierarchical VBR MPEG Video Source Model

Figure 2 shows the general hierarchical structure of the VBR MPEG video source model. It comprises

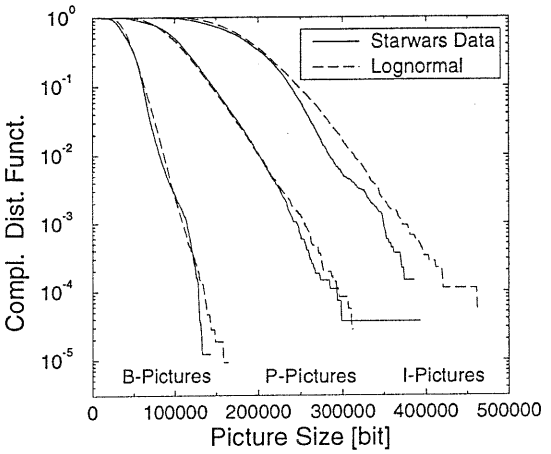

Figure 3: Complementary distribution function of the picture sizes of the 'Starwars' trace

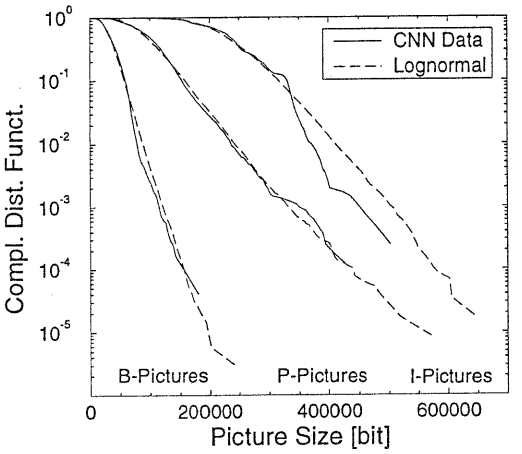

Figure 4: Complementary distribution function of the picture sizes of the 'CNN News' trace

three building blocks representing the behaviour of the source at the scene level, the picture (burst) level and at the cell level. Models describing the encoded video data generally have to take into account the picture size distribution function and the autocorrelation function that are depending on the encoder characteristics and the contents of consecutive pictures. In our model we want to separate the impact of the video contents on the picture sizes from that of the MPEG encoder.

Within the scene activity generation component, the long term fluctuation of the information contents in the video material is characterized. This fluctuation results from object movement, panning and zooming of the camera and scene changes. The picture size generation component specifies the impact of the MPEG coding algorithm on the compression rate that is achieved on consecutive pictures. Finally, the packetization component describes how the coded pictures are packetized into ATM cells and sent to the ATM network.

Cell Level It is assumed that consecutive pictures are completely coded and then packetized into ATM cells. The additional data added by the GOP and video sequence layer is neglected in our model, since it will not change the general behavior of the video data stream. The ATM cells of a picture are transmitted suitably paced over the picture duration $T = 40$ ms.

Picture Level Since the picture sizes are heavily dominated by the GOP structure, the I-, P-, and B-pictures are modelled separately and the picture types are chosen according to the cyclic GOP pattern.

Figures 3 and 4 show the complementary distribution functions of the picture sizes of the 'Starwars' and 'CNN News' statistics traces separately for the I-, P- and B-pictures. As can be seen in both cases, the picture sizes, especially for P- and B-pictures, can be modelled very well by log normal distribution functions fitted by their mean and variance to the experimental data. However, the probability for large I-pictures is somewhat overestimated. The log normal PDF $f_l(y)$ is given by

$$f_l(y) = \frac{1}{\sqrt{2\pi \mathrm{Var}[Z]}} \frac{1}{y} \exp\left[-\frac{1}{2}\frac{(\ln y - \mathrm{E}[Z])^2}{\mathrm{Var}[Z]}\right], \tag{18}$$

with mean $\mathrm{E}[Y] = e^{\mathrm{E}[Z]+\frac{\mathrm{Var}[Z]}{2}}$ and variance $\mathrm{Var}[Y] = e^{(2\mathrm{E}[Z]+\mathrm{Var}[Z])}\,(e^{\mathrm{Var}[Z]} - 1)$ where $\mathrm{E}[Z]$ and $\mathrm{Var}[Z]$ are the mean and variance of the underlying normal PDF.

$X_S(t)$ is a sequence of Gaussian variables with zero mean and unit variance, that will be the output of a ffGn process (see section on scene level below) or a sequence of i.i.d. Gaussian random variables. Let

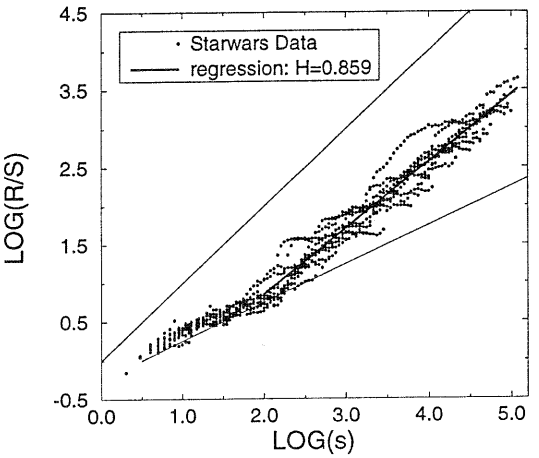

Figure 5: R/S analysis of the 'Starwars' VBR MPEG video trace

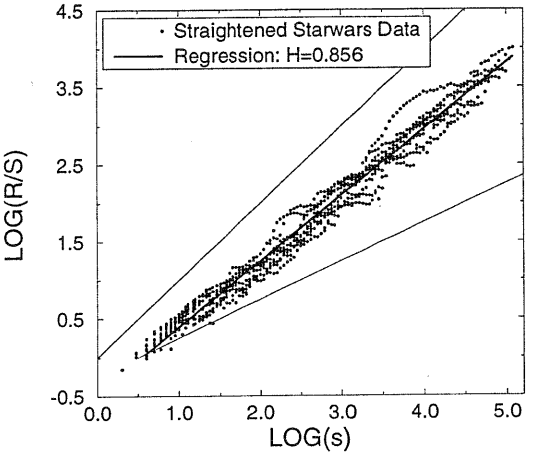

Figure 6: R/S analysis of the straightened out 'Starwars' VBR MPEG video trace

X_i, $i \in \{I, P, B\}$ be the random variable for the I-, P-, and B-picture sizes with $\mathrm{E}[X_i]$ and $\mathrm{Var}[X_i]$ their means and variances as given in table 1. Then, the log normally distributed picture sizes $X(t)$ can be calculated after

$$X(t) = \exp\left[\sqrt{\ln\left(1+\frac{\mathrm{Var}[X_i]}{\mathrm{E}[X_i]^2}\right)}\, X_S(t) + \right. \\ \left. + \ln \mathrm{E}[X_i] - \frac{1}{2}\ln\left(1+\frac{\mathrm{Var}[X_i]}{\mathrm{E}[X_i]^2}\right)\right] , \quad (19)$$

where $i \in \{I, P, B\}$ has to be chosen in compliance with the picture type that the GOP structure prescribes for the picture at time t.

Scene Level A physical explanation for the LRD property exhibited by VBR video traces $\{X_t\}$ arises from the fluctuations in the short term mean $\frac{1}{t_2-t_1}\sum_{t=t_1}^{t_2} X_t$, $1 \le t_1 \le t_2 \le n$, caused by object or camera movement and scene changes [Pott 76] present over a wide range of time scales. Thus the use of a stochastic process exhibiting the LRD property having a single parameter H is a very effective way to model the intensity of the fluctuations in the information contents of consecutive pictures. The Hurst parameter H is estimated from the experimental VBR MPEG video traces using the R/S analysis.

Figure 5 shows the 'pox diagram', i.e. the logarithm of the rescaled adjusted range versus the logarithm of the lag in pictures, for the 'Starwars' picture sizes that exhibit a very long transient up to about a lag of 100 pictures. This is due to the presence of strong cyclic components in the picture size sequence that are introduced by the GOP pattern of the MPEG encoding algorithm. The length of the transient coincides with the mean scene length of about 4 seconds that we found evaluating 25 minutes of the movie. To straighten out the periodic effects of the MPEG encoding algorithm, the inverse of equation 19 can be used on the empirical data to get a sample trace of the supposedly underlying random process. The R/S analysis of the 'Starwars' trace straightened out is depicted in Figure 6. A least squares regression applied to the original and on the straightened data yields in both cases a Hurst parameter of $H = 0.86$ since the asymptotic R/S intensity of dependence is unchanged by the addition of pure sine waves [MaWa 69b] but transient effects are introduced. The Hurst parameter of our 'Starwars' MPEG time series is in good agreement with a Hurst parameter $H = 0.88$ that we found for a 'Starwars' motion JPEG time series and $H = 0.83$ reported in [GaWi 94]. For the 'CNN News' trace we encountered a Hurst parameter of about $H = 0.90$. The higher hurst parameter may result from very sudden changes in the scene activity level switching between head and shoulder scenes and coverage parts.

A discrete fractional Gaussian noise with the appropri-

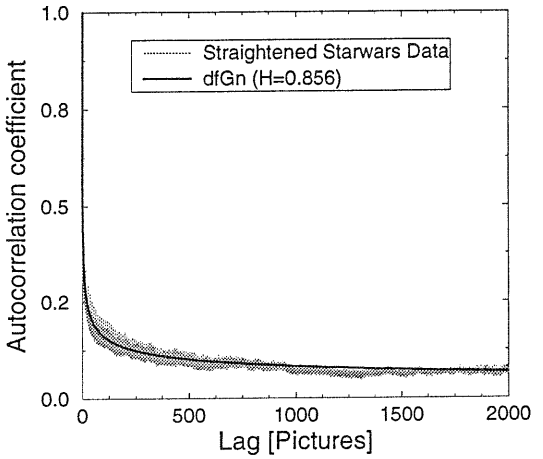

Figure 7: Autocorrelation coefficient of the straightened out 'Starwars' picture size sequence

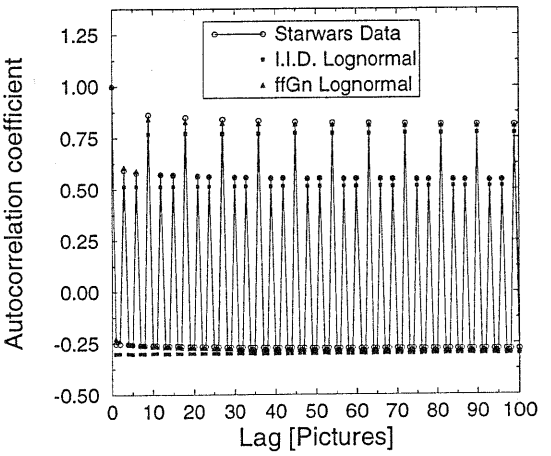

Figure 8: Autocorrelation coefficient of the 'Starwars' picture size sequence

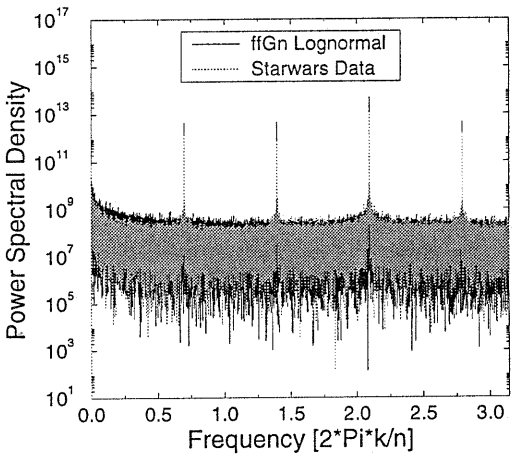

Figure 9: 'Starwars' Periodogram

ate Hurst parameter is very well suited to capture the temporal behaviour of the straightened VBR MPEG video time series. The very good match of the autocorrelation coefficients of the straightened 'Starwars' time series and the corresponding dfGn process (equation 10), even for pictures more than a minute apart, is illustrated in Figure 7. The impact of the LRD scene activity generation process on the correlation structure at the picture level compared to the use of a sequence of independent Gaussian variables is characterized in Figure 8. The autocorrelation structure of the 'Starwars' time series has a decaying component in addition to the periodic constituent imposed by the cyclic GOP structure. Without the LRD process only the periodic constituent is captured [Enss 94]. The dfGn process adds the necessary slowly decaying component to the autocorrelation coefficient of the model.

A summary of the properties of the 'Starwars' time series in the frequency-domain is given in Figure 9 by its power spectral density (periodogram). For low frequencies the frequency spectrum has the form of a power law of the form $\omega_k^{-\alpha}$ characteristic for LRD processes. The four outstanding frequencies correspond to period lengths of 2.25, 3.00, 4.50 and 9.00 pictures. These are the base frequencies that shape the cyclic GOP pattern. The conformity of the power spectral density of the experimental time series with that of our two level model based on an ffGn process and a cyclic nonlinear transform on its output verifies the validity of this approach in the frequency domain.

Multiplexer Model

In order to investigate the feasibility and efficiency of the transmission of VBR video traffic in future ATM systems, understanding the behavior of a multiplexer and its performance is essential. The ATM statistical multiplexer is modelled as a queue with deterministic service time D, a maximum queue size of S cells and

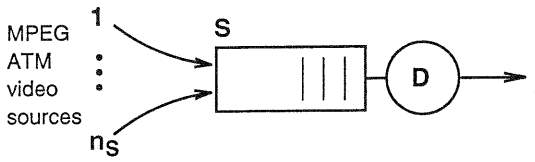

Figure 10: ATM multiplexer model

a link capacity of C Mbit/s that is fed by n_S MPEG ATM video sources (Figure 10).

MULTIPLEXER PERFORMANCE

In this section we want to evaluate the quality of the VBR MPEG video source model and investigate the multiplexing behavior of a number of such sources in terms of cell losses using the multiplexer model presented above. The use of the ffGn scene activity model adds considerable complexity to the overall source model compared to the use of a sequence of i.i.d. random variables. Therefore, it has to be appraised when the more complex ffGn model is necessary and in what cases a simplified model of the picture and cell level is sufficient. In the following it is assumed that the 53 byte ATM cells have a video payload of 47 bytes. All simulation results are given with 95% confidence intervals based on 10 very long simulation part tests. Although, due to the LRD property of the video data, these part tests are not completely independent, they were chosen so long that the remaining correlation is very small. For that reason the confidence intervals are not exact in a rigorous mathematical sense but give a relative bound on the accuracy of the results.

All results will be given for the 'Starwars' data. For the 'CNN News' data we obtained very similar results where for the same load more cell losses were encountered due to the higher Hurst parameter and the larger variance of the picture sizes.

Figures 11 and 12 depict the cell loss probability encountered by a single VBR MPEG video source in a multiplexer depending on the buffer size. The output link of the multiplexer has a transmission capacity of $C = 2.12$ Mbit/s and the source generates a relative load of approximately 0.939. The load of the multiplexer was set pretty high so that the results for all the simulations could be obtained by a current engineering workstation in reasonable time. If the load is lower, the basic behavior of the system stays the same but fewer cell losses will occur. As long as the buffer of the multiplexer can hold less than about 100 cells, a simple model without taking the scene activity level into account is in very good agreement with the results obtained with the 'Starwars' time series. If the buffer is made larger, the simple model underestimates the cell losses by several orders of magnitude, whereas the ffGn model captures the behavior of the empirical

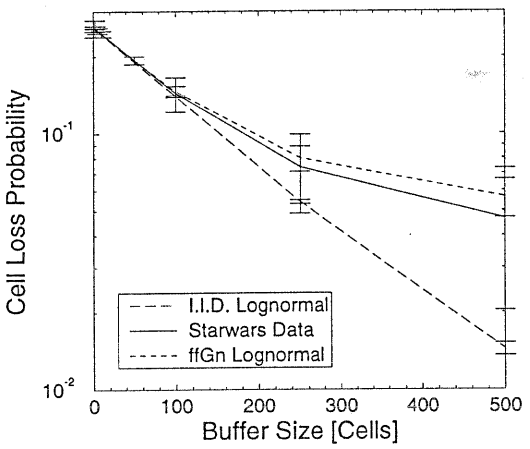

Figure 11: Cell loss probability of a single video source in a multiplexer with small buffer ($C = 2.12$Mbit/s, load 0.939, 95% c. i.)

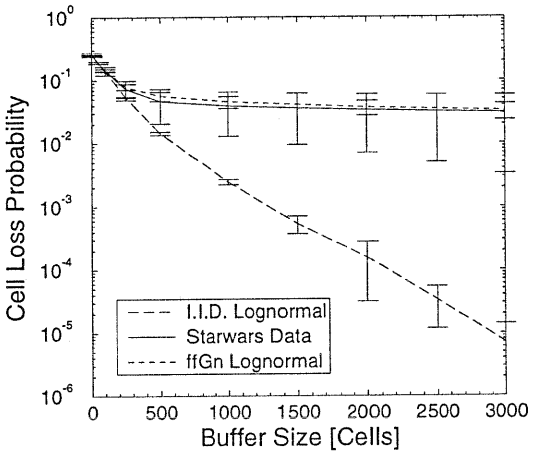

Figure 12: Cell loss probability of a single video source in a multiplexer with large buffer ($C = 2.12$Mbit/s, load 0.939, 95% c. i.)

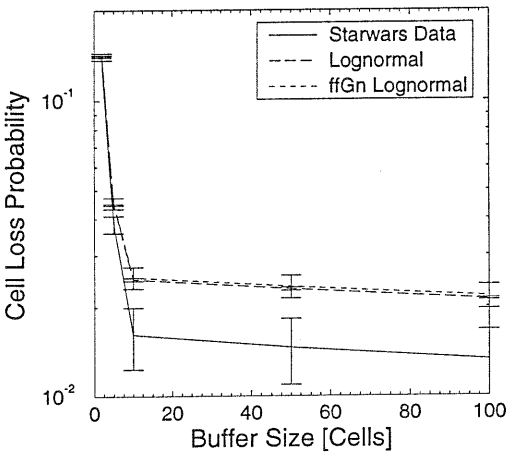

Figure 13: Cell loss probability of 40 video sources in a multiplexer with small buffer (C = 88Mbit/s, load 0.909, 95% c. i.)

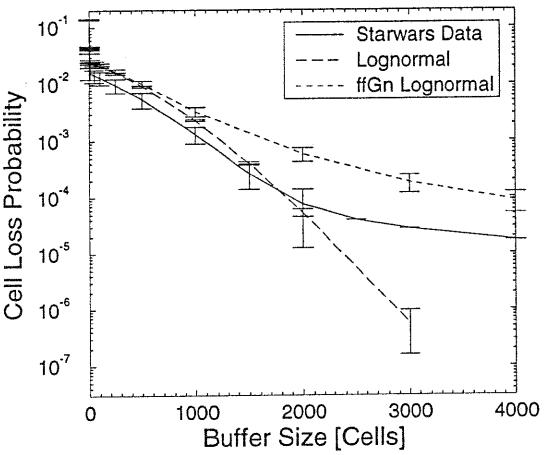

Figure 14: Cell loss probability of 40 video sources in a multiplexer with large buffer (C = 88Mbit/s, load 0.909, 95% c. i.)

'Starwars' time series very well since the LRD property becomes more and more dominant causing a particularly slow decay of the cell loss probability for large buffers.

The cell loss probabilities encountered by 40 VBR MPEG video sources in a multiplexer are illustrated in Figures 13 and 14. The transmission capacity of the multiplexer is C = 88 Mbit/s and the load imposed by the 40 sources is about 0.909. Since the cyclic GOP pattern of the MPEG encoding algorithm has a strong impact on the coded picture sizes the phase relation among the 40 sources is essential for the overall cell loss rate. Therefore the point of time, where the different video sequences start, was chosen randomly within the period of the GOP pattern that is in our case within 360 ms. For small buffers the well known behavior resulting from cell and burst (picture) level fluctuations in the cell arrivals is encountered [KTB 90]. It can be approximated by an M/D/1/S queueing system and a fluid flow approximation [Enss 94]. For large buffers the LRD impact becomes more and more important slowing down the decay of the cell loss rate with increasing buffer size. The ffGn models capture this effect. Again, the simple model, not modelling the LRD property, will underestimate the cell losses for large buffers. However, compared to the 'Starwars' time series, the models should generally somewhat overestimate the losses since the probability for large I-pictures is overestimated by the fitted log normal distribution function.

CONCLUSION

We have investigated the statistical properties of different VBR MPEG video time series. A three level source model, based on a discrete fractional Gaussian noise process and log normal distribution functions for the I-, P-, and B-picture sizes, was presented that captures the essential properties of the encoded video data at the different time scales. The scene level behavior is captured by a single parameter H, the Hurst parameter. The picture level behavior is represented by the means and variances of the picture sizes of the I-, P, and B-pictures. Further, the multiplexing behavior of a number of VBR MPEG video sources was studied. The results of the simulation model including the LRD properties of the video data were found to be in good agreement with simulations driven by the 'Starwars' and 'CNN News' statistics traces over a wide range of buffer sizes.

Generally, the complexity necessary to model VBR MPEG encoded video data depends on the ability of the system under investigation to memorise part of the data stream. The performance of technical systems with little memory is little affected by the long term properties of the video data, whereas systems with

large memories have to cope with these long term properties. So video source models for studying systems with little memory may be far simpler than for systems with large memory. Still an open issue and a topic of further research is the analytical treatment of a multiplexer fed by a number of sources exhibiting LRD properties.

ACKNOWLEDGEMENT

The author would like to thank H. Schultze for the implementation of the ffGn random number generator.

REFERENCES

[Cox 84] D. R. Cox, *Long-Range Dependence: A Review*, Statistics: An Appraisal, Proceedings 50th Anniversary Conference Iowa Stata Statistical Laboratory, H. A. David and H. T. David (Editors), The Iowa State University Press, 1984, pp. 55–74.

[Enss 94] J. Enssle, *Modelling and Statistical Multiplexing of VBR MPEG Compressed Video in ATM Networks*, Proceedings of the 4th Open Workshop on High Speed Networks, Brest, France, September 7–9, 1994, pp. 59–67.

[Fell 51] W. Feller, *The Asymptotic Distribution of the Range of Sums of Independent Random Variables*, The Annals of Mathematical Statistics, Vol. 22, 1951, pp. 427–432.

[Gall 91] D. Le Gall, *MPEG: A Video Compression Standard for Multimedia Applications*, Communications of the ACM, Vol. 34, No. 4, April 1991, pp. 46–58.

[Garr 91] M. W. Garrett, M. Vetterli, *Congestion Control Strategies for Packet Video*, Proceedings of the Fourth International Workshop on Packet Video, Kyoto, Japan, August 1991.

[GaWi 94] M. W. Garrett, W. Willinger, *Analysis, Modeling and Generation of Self-Similar VBR Video Traffic*, ACM SigComm, London, Sept. 1994.

[Hosk 84] J. R. M. Hosking, *Modeling Persistence In Hydrological Time Series Using Fractional Differencing*, Water Resources Research, Vol. 20, No. 12, 1984, pp. 1898–1908.

[Hurs 51] H. E. Hurst, *Long-Term Storage Capacity of Reservoirs*, Trans. Amer. Soc. Civil Eng., Vol. 116, pp. 770–799, 1951.

[KTB 90] H. Kröner, T. H. Theimer, U. Briem, *Queueing Models for ATM Systems — A Comparison*, Proceedings of the 7th ITC Specialist Seminar, Morristown, NJ, October 1990, paper 9.1.

[Magl 88] B. Maglaris, D. Anastassiou, P. Sen, G.Karlsson, J. Robbins, *Performance Models of Statistical Multiplexing in Packet Video Communications*, IEEE Transactions on Communications, Vol. 36, No. 7, July 1988, pp. 834–843.

[MaWa 69a] B.B. Mandelbrot, J. R. Wallis, *Computer Experiments with Fractional Gaussian Noises. Parts 1–3*, Water Resources Research, Vol. 5, No. 1, 1969, pp. 228–267.

[MaWa 69b] B.B. Mandelbrot, J. R. Wallis, *Robustness of the Rescaled Range R/S in the Measurement of Noncyclic Long Run Statistical Dependence*, Water Resources Research, Vol. 5, No. 5, 1969, pp. 967–988.

[Mand 71] B. B. Mandelbrot, *A Fast Fractional Gaussian Noise Generator*, Water Resources Research, Vol. 7, No. 3, 1971, pp. 543–553.

[MPEG 92] Draft International Standard ISO/ IEC DIS 11172, *Information technology — Coding of moving pictures and associated audio for digital storage media up to about 1.5 Mbit/s*, 1992.

[MRSZ 92] B. Melamed, D. Raychaudhuri, B. Sengupta, J. Zdepski, *TES-Based Traffic Modeling For Performance Evaluation Of Integrated Networks*, Proceedings of INFOCOM '92, Florence, Italy, May 1992, pp. 75–84.

[NFO 89] M. Nomura, T. Fujii, N. Ohta, *Basic Characteristics of Variable Rate Video Coding in ATM Environment*, JSAC Vol. 7, No. 5, June 1989, pp. 752–760.

[PaZa 92] P. Pancha, M. El Zarki, *A Look at the MPEG Video Coding Standard for Variable Bit Rate Video Tramsmission*, Proceedings of INFOCOM '92, Florence, Italy, May 6–8, 1992, pp. 85–94.

[PaZa 93] P. Pancha, M. El Zarki, *Bandwidth Requirements of Variable Bit Rate MPEG Sources in ATM Networks*, Proceedings of INFOCOM '93, San Francisco, CA, March 30 – April 1, 1993, pp. 902–909.

[Pott 76] K. W. Potter, *Evidence for Nonstationarity as a Physical Explanation of the Hurst Phenomenon*, Water Resources Research, Vol. 12, No. 5, 1976, pp. 1047–1052.

[RaSe 90] G. Ramamurthy, B. Sengupta, *Modelling and Analysis of a Variable Bit Rate Video Multiplexer*, Proceedings of the 7th ITC Specialist Seminar, Morristown, NJ, October 1990, paper 8.4.

[Rein 93] D. Reininger et al, *Statistical Multiplexing of VBR MPEG Compressed Video on ATM Networks*, Proceedings of INFOCOM '93, San Francisco, CA, March 30 – April 1, 1993, pp. 919–926.

[SSD 93] P. Skelly, M. Schwartz, S. Dixit, *A Histogramm-Based Model for Video Traffic Behavior in an ATM Multiplexer*, IEEE/ACM Transactions on Networking, Vol. 1, No. 4, August 1993, pp. 446–459.

[VPV 88] W. Verbiest, L. Pinnoo, B. Voeten, *The Impact of the ATM Concept on Video Coding*, JSAC, Vol. 6, No. 9, 1988, pp. 1623–1632.

[WaMa 70] J. R. Wallis, N. C. Matalas, *Small Sample Properties of H and K — Estimators of the Hurst Coefficient h*, Water Resources Research, Vol. 6, No. 6, 1970, pp. 1583–1594.